

See discussions, stats, and author profiles for this publication at: <https://www.researchgate.net/publication/242253525>

# Survey of results on plasma biasing in the CASTOR tokamak

Article · January 2007

CITATIONS

0

READS

19

12 authors, including:



**J. Stockel**

The Czech Academy of Sciences

259 PUBLICATIONS 1,698 CITATIONS

[SEE PROFILE](#)



**Jiri Adamek**

The Czech Academy of Sciences

143 PUBLICATIONS 1,383 CITATIONS

[SEE PROFILE](#)



**Jana Brotánková**

Czech Technical University in Prague

51 PUBLICATIONS 521 CITATIONS

[SEE PROFILE](#)



**R. Dejarnac**

The Czech Academy of Sciences

111 PUBLICATIONS 707 CITATIONS

[SEE PROFILE](#)

Some of the authors of this publication are also working on these related projects:



Physics of plasma [View project](#)



Installation of new divertor ball-pen and Langmuir probes on the COMPASS tokamak. [View project](#)

## Survey of results on plasma biasing in the CASTOR tokamak

J Stockel<sup>1</sup>, J Adamek<sup>1</sup>, J Brotánková<sup>1</sup>, R Dejarnac<sup>1</sup>, P Devynck<sup>2</sup>, I Duran<sup>1</sup>, J Gunn<sup>2</sup>, J Horacek<sup>1</sup>, M Hron<sup>1</sup>, M Kocan<sup>2</sup>, E Martinez<sup>3</sup>, R Panek<sup>1</sup>, M Spolaore<sup>3</sup>, G Van Oost<sup>5</sup>

<sup>1</sup>Institute of Plasma Physics, Association EURATOM-IPP.CR, Prague, Czech Republic

<sup>2</sup>Association EURATOM-CEA sur la fusion contrôlée, Saint Paul Lez Durance, France

<sup>3</sup>Consorzio RFX, Associazione EURATOM-ENEA sulla Fusione, Padova, Italy

<sup>5</sup>Department of Applied Physics, Ghent University, Ghent, Belgium

### Abstract

Experimental observations on edge plasma biasing on the CASTOR tokamak are summarized. Three regimes differing in the electrode position and in the biasing voltage are identified. Characteristic features observed at the plasma edge are studied by a set of electric probes and impact of biasing on the edge plasma as well as on global confinement is described.

### Experimental set-up

Plasma biasing experiments are performed on the CASTOR tokamak ( $R=0.4$  m,  $a = 85$  mm,  $B_T = 1.3$  T,  $I_p \approx 10$  kA,  $n_e \approx 10^{19}$  m<sup>-3</sup>). The arrangement of the biasing experiment is schematically shown in Fig. 1. Because of the downward shift of the plasma column, the edge plasma is divided into three regions, regarding the parallel connection length  $L$  to a material surface, which is represented by the poloidal limiter:

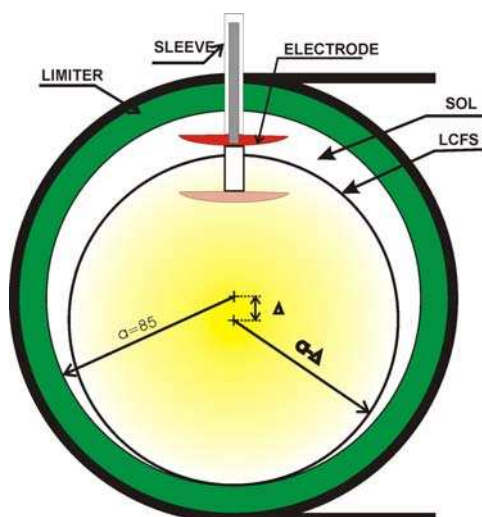


Fig. 1 Experimental set-up

- *Limiter shadow* is the region between the chamber wall and the leading edge of the poloidal limiter ( $85 \text{ mm} < r < 100 \text{ mm}$ ). The corresponding connection length is about one toroidal circumference,  $L \sim 2\pi R$ .
- *Scrape-off layer (SOL)* with a much longer connection length is formed at the upper part of the plasma column because of the vertical shift of the plasma. The connection length  $L \sim q2\pi R$  is proportional to the local safety factor  $q$  (typically  $q = 6-9$  in CASTOR). The radial extent of the SOL is largest at the top of the torus and depends on the value of plasma displacement.
- *Confinement region* with an infinite connection length.

The biasing electrode is inserted into the plasma from the top of the torus as shown in Fig. 1 either in the confinement region or in the SOL. The edge plasma is diagnosed by a set of electric probes to measure the radial profiles of plasma density and temperature, their poloidal distribution, ion flow velocity, and other parameters of interest [1].

### Results

Three distinct and reproducible regimes have been identified with this arrangement:

1) Electrode is inserted within the LCFS and biased to +100-150 V; A transition to a regime with improved particle confinement is routinely observed as evident from Fig.2 (left panel). The line average density increases and the recycling is reduced (a drop of the  $H_{\alpha}$  intensity) during the biasing period. Simultaneously, steepening of the radial profiles of the plasma density and potential just inside the LCFS indicates formation of a transport barrier in this region.

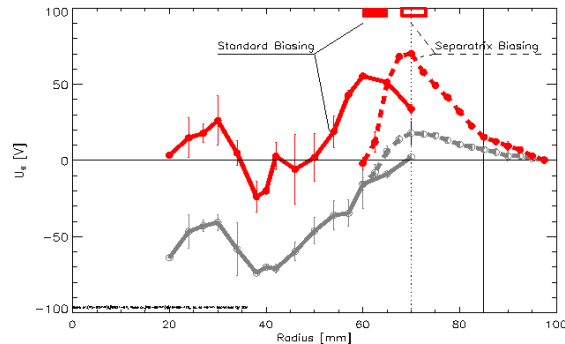
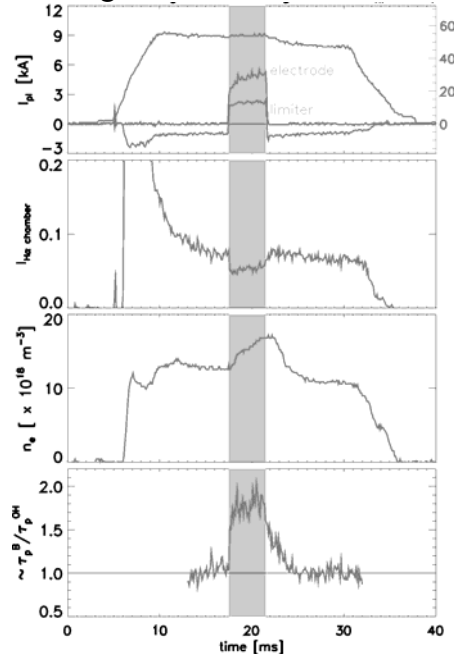


Fig 2. Left – Evolution of a discharge with biasing; Right – radial profile of the floating potential for two positions of the biasing electrode; red solid line – electrode is inside the LCFS, red dashed line – electrode is inside the SOL. The ohmic profile is shown for comparison by gray lines.

Furthermore, the radial electric field is amplified, the ion flow velocity increases and the edge turbulence is reduced [2].

Measurements of the radial profile of the floating potential (full red line in Fig. 2 –right) show that the whole plasma column is biased to the voltage applied to the electrode. A quite different profile of  $U_{\text{fl}}$  is observed if the electrode is located within the SOL.

2) Electrode is inserted deep into the plasma ( $r/a < 0.5$ ) and biased to a higher voltage +250-300V; The transport barrier in front of the LCFS becomes unstable and relaxes quasi-periodically with a frequency of about 10 kHz. However, the global particle confinement remains still improved. Detail description is given in [3,4]. Here, we emphasize just a result obtained with a probe array, which consists of two rows of Langmuir probes. Such probe head (shown in Fig. 3) is exploited to study 2D structure of the edge electric field.



Fig. 3. Photograph of the double rake probe. Two rows of Langmuir tips are spaced poloidally by 2.5 mm. The radial distance between the tips is also 2.5 mm. The individual tips measure either the floating potential or the ion saturation current. The mode of operation can be changed between shots. Signals are recorded with the sampling frequency 1 MHz

The result of monitoring of the electric field during the relaxation period of a biased discharge is shown in Fig. 4. The top panel shows the evolution of the *radial* electric field. The radial electric field reaches periodically values up to 25 kV/m within a highly sheared region of a radial width of about 1 cm (bright yellow spots), which is associated with the position of the transport barrier. Furthermore, it is evident that the barrier propagates radially outward as emphasized by the dashed line. The propagation velocity is estimated as  $\sim 0.2$

km/s. As the propagation velocity is quite constant, the exact frequency of the relaxations (around 10kHz) was found experimentally [4] to be determined by the propagation time from the electrode position to the LCFS ( $r_{LCFS} = 65$  mm in this particular case) where the barrier collapses. Moreover, it is evident that the radial width of the transport barrier becomes narrower when it is approaching the LCFS.

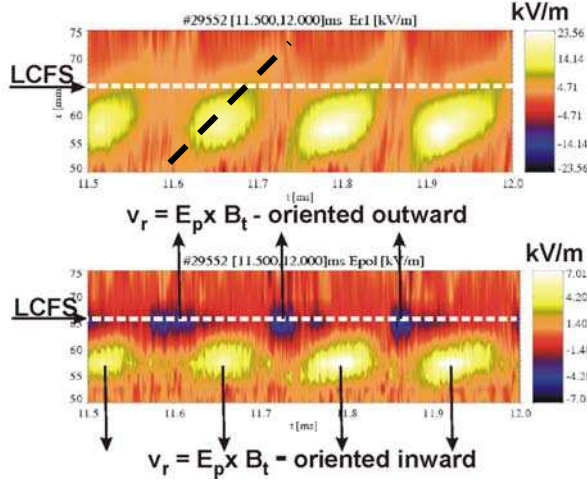


Fig. 4: Temporal evolution of the radial profiles of the radial (top panel) and poloidal (bottom panel) component of the electric field during the biasing phase. Position of the LCFS is 65 mm in this case.

The radial electric field is calculated as a difference of floating potentials of the radially spaced tips, the poloidal component of  $E$  is derived in a similar way from signals of poloidally spaced tips. The gradient of electron temperature is not taken into account.

It is clearly seen from the bottom panel of Fig. 4 that a significant poloidal component of the electric field (bright yellow patterns) forms within the transport barrier as well. The position of the region with the amplified poloidal field,  $E_p$ , corresponds to that of the radial component. Its radial width appears to be narrower than that of  $E_r$ . It should be also noted that the amplitude of  $E_p$  is significantly smaller than the radial component,  $E_r \sim 3E_p$ . The resulting  $E_p \times B_t$  velocity is oriented inward, i.e. the radial drift contributes to steepening of density profiles. On the other hand, the poloidal electric field of the opposite sign is formed during the collapse of the transport barrier, as marked by dark blue spots. This region of  $E_p$  is quite narrow and localized almost exactly at the LCFS. The corresponding  $E_p \times B_t$  velocity and the resulting radial flux are oriented outward. The outward convection of the edge plasma is manifested by bursts in the temporal evolution of the ion saturation current [3].

3) Electrode is localized in the SOL; In contrast to the previous arrangement, only a narrow region associated with the electrode position is biased, as already shown in Fig. 2 by the red dashed line. Moreover, the increase of the plasma potential is not poloidally uniform, which is manifested in Fig 5, where the poloidal distribution of the floating potential is plotted.

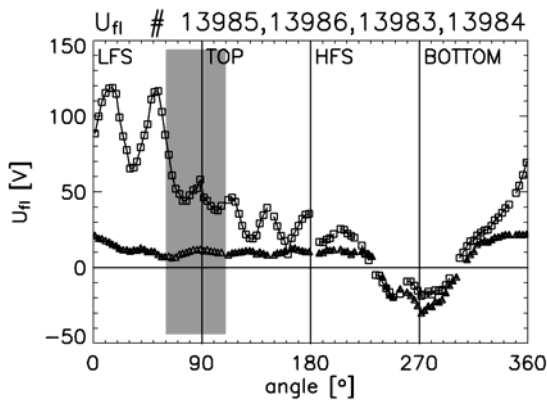


Fig 5. Poloidal distribution of the mean floating potential  $U_{fl}$  along the poloidal array of Langmuir probes in ohmic (triangles) and biasing (squares) phase, as measured in four reproducible discharges with a constant edge safety factor  $q(a) \sim 8$ . The poloidal position of the biasing electrode is marked by the grey bar.

Peaks of the floating potential observed in the range of poloidal angles  $0^\circ$ - $200^\circ$  are interpreted as a projection of a biased flux tube on the poloidal array of probes surrounding

the plasma column [5]. The biased flux tube originates at the electrode and extends along the helical magnetic field line. The electrode current flows predominantly parallel to the magnetic field lines in the upstream and downstream direction and terminates on the electron and ion side of the bottom part of the poloidal limiter. Therefore, the resulting electric field has not only a radial, but also a *poloidal* component. Its sign changes with the poloidal angle. Consequently, a convective motion of the SOL plasma occurs because of the  $E_{\text{pol}} \times B_t$  drift, directed either inward or outward according the sign of the  $E_{\text{pol}}$ . The convective particle flux (see left panel of Fig. 6) dominates in the SOL since it is by two orders of magnitude larger than the fluctuation-induced one.

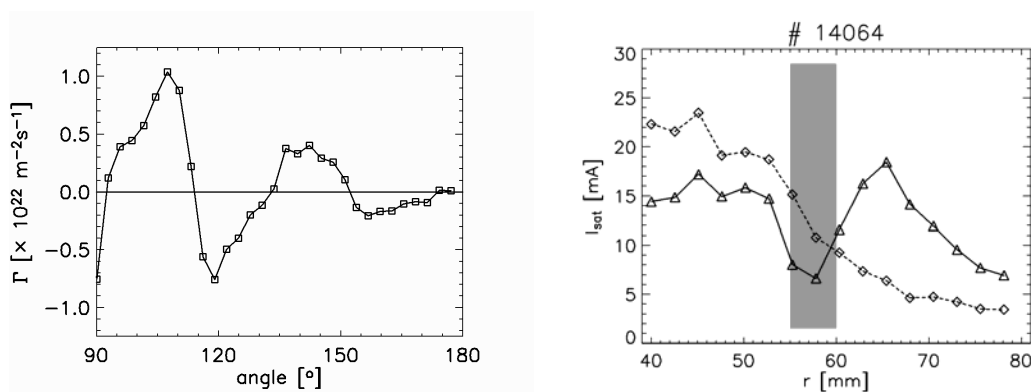


Fig. 6. Left - Distribution of the radial particle flux driven by the poloidal electric field along one quarter of the poloidal circumference (high field side – top). Right - Comparison of the radial profile of the ion saturation current in the ohmic (dashed line) and in the SOL biasing (solid line) phase of the discharge. The gray bar marks the electrode position.

The strong effect on the SOL equilibrium profile is further confirmed by measurements of the radial profile of the ion saturation current, obtained using the rake probe. Such measurements are shown in the right panel of Fig. 6, both for the ohmic phase and during the SOL biasing. The density profile displays a strong depletion at the location of the electrode during the biasing phase. The density in front of this position is also reduced, whereas a density accumulation can be seen in the region between 60 and 70 mm, behind the electrode. This strong modification of the density profile is consistent with an increase of the particle flux at the radial location where the electrode is placed.

#### References

1. J Stockel et al, Journal of Physics, Conference Series, 63 (2007), 012001
2. G Van Oost, et al: In Proc. of 28<sup>th</sup> EPS Conference on Contr. Fusion and Plasma Phys, Funchal, Portugal, European Conference Abstracts ECA Vol. 25A (2001), 1665
3. M Spolaore et al, Czech.J.Phys., 55 (2005), No. 12, 1597-1606
4. J Stockel et al, Problems of Atomic Science and Technology: Plasma Physics, 2006, No,6, 19-23, [http://vant.kipt.kharkov.ua/CONTENTS/CONTENTS\\_2006\\_6.html](http://vant.kipt.kharkov.ua/CONTENTS/CONTENTS_2006_6.html)
5. J Stockel et al, Plasma Phys. Contr. Fusion, 47, 2005, 635-643

#### Acknowledgement

This research is supported by the grant GA AV B100430602 and by the INTAS project Nr 5 100008-8046. Jan Horacek acknowledges support from the European Atomic Energy Community under an intra-European fellowship (EURATOM).